Technologia i Automatyzacja Montażu

Volume 126, Issue 4/2024, Pages 3-13
https://doi.org/10.7862/tiam.2024.4.1

Original Research

STRENGTH TESTS OF REPAIR JOINTS LOADED WITH TENSION AND LOSS OF STABILITY

BADANIA WYTRZYMAŁOŚCI WĘZŁÓW NAPRAWCZYCH OBCIĄŻONYCH NA ROZCIĄGANIE I UTRATĘ STATECZNOŚCI

Iga BARCA[1,*], Jan GODZIMIRSKI[1], Marek ROŚKOWICZ[1]

[1] Faculty of Mechatronics, Armament and Aerospace, Military University of Technology, Warsaw, Poland

* Corresponding author: iga.barca@wat.edu.pl

Abstract

During aircraft service, the skin is the component that first comes into contact with factors that can cause mechanical damage - that is why it is most often damaged during use. Semi-monocoque aircraft structures are made of a skin and a frame. The skin is an element that significantly affects the safety of the structure, since it transfers loads between the elements of the frame. For this reason, the skin is subject to special supervision during technical maintenance, and any damage detected must be repaired. The research was carried out on specimens made of AW 2024-T3 plate sheet with a thickness of 1 mm. In the study, a comparative analysis of damaged, undamaged and repaired specimens loaded in tension and compression was performed. Different patches were used in repaired specimens, made of metallic as well as composite materials, connected to the structure with rivets or using adhesive materials. The study showed that the use of riveted as well as adhesively bonded overlays does not allow the original strength of the tensile-loaded skin to be restored, but does allow the strength of the compression-loaded skin to be restored. In addition, numerical simulations were performed to define the stress field occurring in the adhesive joint for different geometric dimensions of the plate. The results of the numerical analysis showed that the geometry of the plate model influences the values of reduced stresses in the adhesive weld and the patch. Regardless of the analyzed changes in the geometry of the plate model, the maximum values of reduced stresses are similar to each other. The smallest values of reduced stresses in the adhesive joint and composite patch were obtained for the case of a plate with a thickness of 1 mm and a width of 160 mm.

Keywords: repair node, semi-monocoque structure, composite materials, numerical calculations

Streszczenie

Podczas eksploatacji statków powietrznych pokrycie jest elementem, który w pierwszej kolejności ma kontakt z czynnikami mogącymi wywołać uszkodzenie mechaniczne – stąd najczęściej ulega uszkodzeniu podczas eksploatacji. Konstrukcje półskorupowe statków powietrznych wykonane są z pokrycia i szkieletu. Pokrycie jest elementem, który istotnie wpływa na bezpieczeństwo konstrukcji, ponieważ przenosi obciążenia pomiędzy elementami szkieletu. Z tego powodu pokrycie podlega szczególnemu dozorowi podczas przeglądów technicznych, a wykryte uszkodzenia muszą być naprawione. Badania prowadzono na próbkach wykonanych z arkusza blachy AW 2024-T3 o grubości 1 mm. W pracy wykonano analizę porównawczą próbek uszkodzonych, nieuszkodzonych i naprawionych próbkach obciążanych na rozciąganie i ściskanie. W próbkach naprawianych zastosowano różne nakładki, wykonane z materiałów metalowych jak i kompozytowych, łączonych ze strukturą nitami lub z wykorzystaniem tworzyw adhezyjnych. Badania wykazały, że zastosowanie nakładek nitowanych jak i klejonych nie umożliwiają odtworzenia pierwotnej wytrzymałości pokrycia obciążonego na rozciągania, ale umożliwiają odtworzenie wytrzymałości pokrycia obciążonego na ściskanie. Dodatkowo wykonano symulacje numeryczne, w celu zdefiniowania pola naprężeń występujących w spoinie klejowej dla różnych wymiarów geometrycznych płyty. Wyniki analizy numerycznej wykazały, że geometria modelu płyty wpływa na wartości naprężeń zredukowanych w spoinie klejowej i nakładce. Niezależnie od analizowanych zmian w geometrii modelu płyty maksymalne wartości naprężeń zredukowanych są do siebie zbliżone. Najmniejsze wartości naprężeń zredukowanych w spoinie klejowej oraz nakładce kompozytowej otrzymano dla przypadku płyty o grubości 1 mm i szerokości 160 mm.

Słowa kluczowe: węzeł naprawczy, konstrukcja półskorupowa, kompozyt, obliczenia numeryczne

1. Introduction

Semi-monocoque structures have been a common design solution for aircraft airframes for many years (Motley, 1980). Semi-monocoque designs are made of a skin and a frame, and both the frame and the skin carry the loads caused by external forces (Hoff, 1946). In the past, in beam structures, the skin was made of fabric (Akash et al., 2017; Al-Rabeei, 2024), and at that time it was not as important structural element as moder skin made of aluminum alloys or composite materials (Azmin et al., 2012).

The formula of semi-monocoque structure can be used to make wings, fuselage or aircraft aileron, and the strain on these elements is caused by the presence at the same time shearing forces, bending moments and torsional moments, which consequently cause a complex state of stress, in the elements of the frame and in the skin (Siddiqui, 2014; Kołodziejczyk and Święch, 2018). In particular, the aircraft skin is the component that first comes into contact with factors that can cause mechanical damage to the structure – thus it is most often damaged during aircraft life (Cantwell and Morton, 1992; Henaff et al., 2019).

Making repairs to the skin is an important aspect that affects the safety of the structure, since the skin is also a component that transfers loads between framing members, including stringers, spars and ribs. Damage to the skin impacts to the stress distribution in the skin itself, but also in the adjacent framing elements and in the connections occurring between the skin and the frame. The consequence of primary damage to the skin can be further propagation of damage to adjacent elements and secondary damage. For this reason, the skin is particularly subject to supervision during technical inspections (Bazargan, 2010), and detected damage to the skin must be repaired to maintain its integrity and restore the original strength of the damaged component (Chang and Zang, 2023; Armstrong et al., 2005; Dai et al., 2020].

Repairs of metallic aircraft structures using composite materials and adhesive materials were initiated in 1970 (Baker, 1984; Baker 1999; Baker and Joned, 1988). It is not a widely used method in the repair of metallic aircraft structures, due primarily to the challenges associated with the certification process. However, considering: the favorable time-consumption of the adhesive repair process (practically defined by the crosslinking time of structural adhesive materials), the durability of the repair and, above all, the lack of the need for additional secondary damage (mounting holes), repairs of aircraft structures using composite patches and adhesive bonds are still being developed. (Hamill and Nutt, 2018; Rośkowicz and Smal, 2012).

The classic solution for installing repair patches is to use mechanical fasteners in the form of, for example, rivets (Camanho and Lambert, 2006). The main disadvantage of this type of solution, as previously mentioned, is the additional local "weakening" of a section of the undamaged skin by making mounting holes (Camanho and Matthews, 1999). However, based on research, it has been shown that repairs using adhesive materials have a number of advantages over the traditional repair method in which mechanical fasteners are used, such as lighter weight, more streamlined shape, ability to reproduce more complicated shapes, reduction of stress concentration around the repair node (Ma et al., 2021, Megueni and Yala, 2009) and effective load transfer especially in thin-walled parts (Ayedi et al., 2014, Gan et al., 2006). Repair of skin elements can be made by cutting a hole in the shape of a circle, triangle, rectangle, trapezoid, ellipse and octagon. At the site of the damage, after removing a section of the skin, an insert reproducing the cut hole can be installed in the made hole, and an patch is installed to ensure the tightness of the repair node and restore locally the strength and stiffness parameters of the damaged element (Barca and Rośkowicz, 2022).

Publication (Khazaei et al., 2021) analyzed the effect of the patch material used on the restoration of the original strength of the repaired structure, and publication (Bond and Maxwell, 1999) studied the effect of the type of repair used with symmetrical and asymmetrical composite patches on the stress intensity factor during fatigue testing. The study showed that the type of symmetric and asymmetric patches used significantly affects the fatigue life of the repaired metal plate.

Other publications (Prakash et al., 2013; Albedah et al., 2021; Lee et al., 2021; Gunnion and Wang, 2009) analyzed the effect of the applied patch shapes in the repair node on the values of the stress intensity factor. It was shown that its greatest decrease occurred with octagonal-shaped patches, and that the use of an elliptical patch shape reduces the amount of material removed compared to a circular shape by up to 41% in the repaired structure, and results in a reduction in shear stress in the structure of up to 18% compared to a cut-out circular shape (Shazly, 2021).

So far, there has been a lot of work on performing adhesive repairs using composite materials for the repair of metal skin, semi-monocoque aircraft structures. The publication (Katnam et al., 2013) reviews previous research and analysis on the possibility of using composite materials in primary aircraft structures. The issue of using composite materials in the repair of aviation structures is complicated, if only because of the anisotropic properties of composite

patches or the different, depending on their location in the aircraft structure, dominant loads on the same elements. An example of such an element is the wing skin, which is in tension at the bottom of the wing and compression at the top of the wing.

Therefore, the purpose of this work is to perform a comparative analysis of undamaged, damaged and repaired specimens loaded in tension and compression. The repaired specimens used various patches, made of both metallic and composite materials, connected in the repair zone traditionally with rivets or bonded to the repair nodes with adhesive materials. On the occasion of the realization of comparative studies, numerical simulations were carried out with the aim of defining the stress field occurring in the adhesive joint, that is, in the element most important for the restoration of the original strength and stiffness properties of the skin damage zone (Achour et al., 2013). The main aim was to test the possibilities of repairing metal thin skins of semi-monocoque aircraft structures by applying composite patches.

2. Research methodology

Comparative tests of repair junctions were carried out on specimens made of EN AW2024-T3 aluminum alloy with a 20 mm diameter hole (representation of the so-called small punctures of the skin). The geometric dimensions of the used specimens are presented in Figure 1. Metal inserts also made of EN AW2024-T3 aluminum alloy with a diameter of 20 mm were riveted to the previously prepared repair pads (metal and composite) with a diameter of 70 mm using a rivet ø1.5 mm of PA 25 alloy.

Three types of material were used for composite patches made of:

- Aeroglass 110g/m2 glass fabric made from 10 layers with $[0°;45°]_5$ orientation infused with L285/H285 resin in mass proportions of 100:40 - the obtained patch thickness was equal to 1 mm (GFRP – Glass Fiber Reinforced Polymer);
- carbon composite made by the company (Silesian Science and Technology Center of Aviation Industry Sp z o.o. from 10 layers of GG204T 2x2 Twill 3K prepreg with $[0°;45°]_5$ orientation - the resulting overlay thickness was equal to 1.6 mm (CFRP – Carbon Fiber Reinforced Polymer);
- EN AW-2024-T3 aluminum alloy plates with thicknesses of 0.3, 1 and 2 mm.

The 70 mm diameter patches were bonded to the specimen using adhesives: DP 420 (3M USA) and Loctite 9464 (Henkel Germany). Adhesive materials were selected on the basis of in-house tests, the results of which were presented in the publication (Barca et al., 2023). The surfaces to be bonded were grinded with 3M abrasive discs of 80 grit. As reference specimens, riveted specimens witch patches were also prepared, using 6 rivets of 3.5 mm diameter made of PA 25 aluminum alloy. The geometry of the specimen and the rivet joint is shown in Figure 2. The mounting holes were made with a 3.5 mm drill bit at an angle of 90°. The holes were made at a distance of 10 mm from the edge of the patch. The angle between the holes is 60°. Variants of the fabricated specimens are shown in Table 1 and Figure 3.

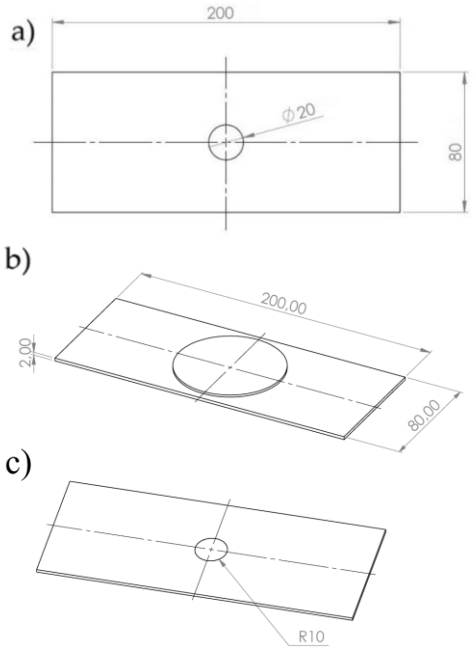

Fig. 1. Geometric dimensions: a) plate with hole, b) repaired specimen (patch ø70 mm), c) repaired specimen (second side with insert ø20 mm)

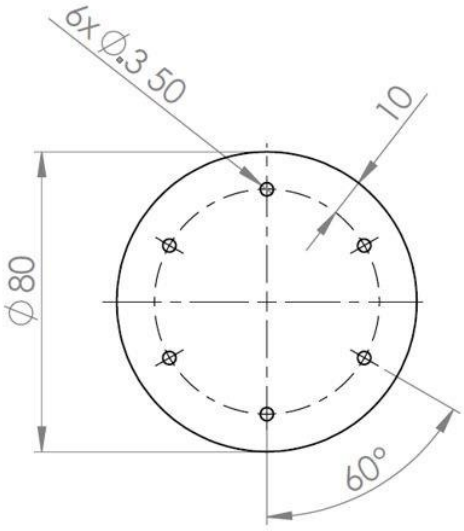

Fig. 2. Geometry of the rivet joint

Table 1. Variants of the specimens made

Specimen No.	Patch material	Patch diameter [mm]	Patch thickness [mm]	Type of patch connection
1.	AW-2024-T3	80	2	mechanical /rivets
2.		70	2	adhesive /DP 420
3.			1	adhesive /DP 420
4.			0.3	adhesive /DP 420
5.	CFRP		1.6	adhesive /DP 420
6.			1.6	adhesive /Loctite 9464
7.	GFPR		1	adhesive /Loctite 9464
8.			1	adhesive /DP 420

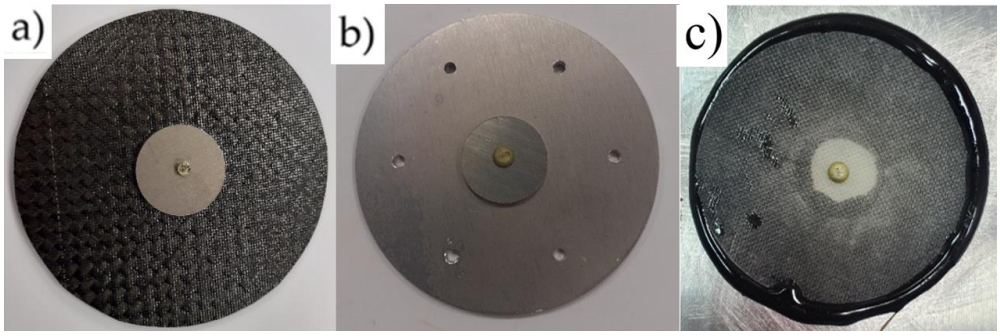

Fig. 3. Prepared patches: a) CFRP, b) aluminum alloy, c) GFRP

The specimens were subjected to tensile and compression tests. Static tests were carried out on a Fritz Heckert ZD10 testing machine at a speed of 2 mm/min. Tensile specimens were fixed in flat jaws, while compression specimens were supported articulated on both sides by placing them in the prismatic grooves of the testing machine's platters. The values of the failure forces for the tension-loaded specimens and the critical force during loss of stability for the compression specimens were recorded.

3. Results and discussion

3.1. Tensile test results

The results of the static tensile tests performed on specimens with repair nodes. For each case, three specimens were tested, the obtained force values of which were averaged and placed in a Table 2. Examples of the failure forms of the tested specimens are shown in Figure 4. In specimens with bonded patches, specimen cracking was observed in the section weakened by the hole. In the case of specimens with riveted patch, damage propagation began at the location of holes prepared for rivets.

Table 2. Tensile test results

Specimen No.	Specimen type	Patch			Force [kN]
		Material	Thickness [mm]	Patch connection type	
1	Undamaged	-	-	-	69.3
2	Damaged	-	-	-	50
3	Repaired	AW-2024-T3	2	mechanical /rivets	46.3
4			2	adhesive /DP 420	49.5
5			1	adhesive /DP 420	53.8
6			0.3	adhesive /DP 420	53
7		CFRP	1.6	adhesive /DP 420	51.2
8			1.6	adhesive /Loctite 9464	50
9		GFRP	1	adhesive /Loctite 9464	50
10			1	adhesive /DP 420	49.5

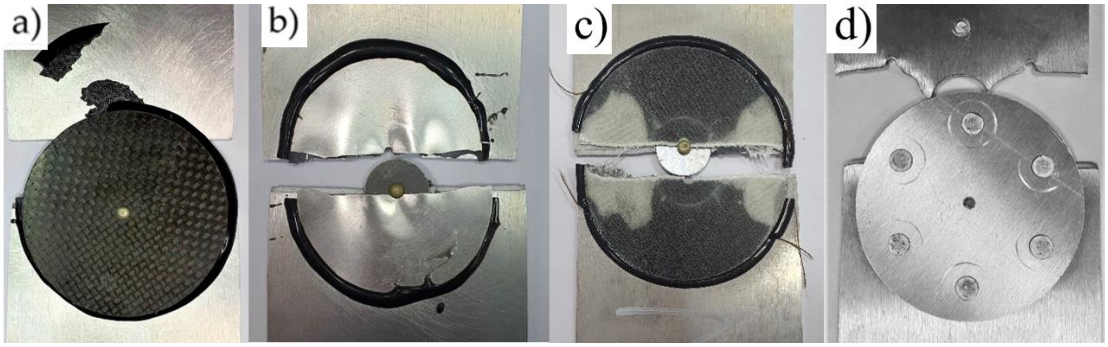

Fig. 4. Photos of failure of tensile specimens with overlay: a) carbon, b) metal thickness = 0.3 mm, c) glass, d) riveted metal thickness = 2 mm.

The form of damage with a hole was related not only to the reduction of the loaded cross-sectional area by the 20 mm diameter hole, but also resulted from the occurrence of the phenomenon of stress concentration in the area of the rivet mounting holes. The failure stresses in the specimen without a hole are:

$$\sigma_n = \frac{F}{A} = \frac{69300}{80 \times 2} = 433\ MPa \qquad (1)$$

While a in a specimen with a hole:

$$\sigma_{no} = \frac{F}{A} = \frac{50000}{60 \times 2} = 416.7\ MPa \qquad (2)$$

The effect of stress concentration at a 20-mm-diameter hole causes a slight decrease in strength of about 4% when the material is deformed in the plastic range. The repair methods used practically did not increase the tensile strength of the specimens. The consequence of the classical repair performed with riveted overlays was a reduction in the failure load of the specimen because the rivet holes as so-called stress concentrators were the places from where the failure process of the specimen probably started (Fig. 4d). When the specimens with stiffer patches (CFRP and AW-2024-T3 with a thickness of 2 mm) were loaded and in the load range of about 30 kN, "crackling" was heard due to the cracking of adhesive joints and the patches themselves did not fail (Fig. 4a). Overlays with lower stiffness (glass composite and AW-2024-T3 with a thickness of 0.3 mm) decohered simultaneously with the repaired specimen (Fig. 4b, Fig. 4c).

3.2. Compression test results

The manner of deformation of the specimens during the compression test is shown in Figure 5. The results of the static compression tests carried out on the specimens with repair nodes. Again, three specimens were tested for each case, and the resulting force values were averaged and placed in a Table 3.

Fig. 5. Specimen loaded with compressive force

Table 3. Results of compression test of specimens

Specimen No.	Specimen type	Patch				Force [kN]
		Material	Diameter [mm]	Thickness [mm]	Patch connection type	
1	Undamaged	-			-	0.75
2	Damaged	-			-	0.7
3	Repaired	AW-2024-T3	80	2	mechanical /rivets	1.18
4			70	2	adhesive /DP 420	1.2
5		CFRP		1.6	adhesive /DP 420	1.53
6				1.6	adhesive /Loctite 9464	2.2
7		GFRP		1	adhesive /Loctite 9464	1.95
8				1	adhesive /DP 420	0.95

Assuming that the test specimens loaded axially along the dominant geometric dimension, behave as jointed supported bars, the critical force value for the undamaged specimen was calculated.

$$F_{critical} = \frac{\pi^2 E \times J}{l^2} \quad (3)$$

$$J = \frac{b \times h^3}{12} = \frac{80 \times 2^3}{12} = 53.3\ mm^4 \quad (4)$$

$$F_{critical} = \frac{\pi^2 70000 \times 53.3}{210^2} = 835\ N \quad (5)$$

The calculated value of the critical force for the specimen without a hole was greater than the experimentally defined value by 10%.

The critical force for the specimen with the hole was about 7% less than the critical force of the undamaged specimen. Each of the repair methods used resulted an increase in the critical force of the repaired specimens compared to the critical force of the undamaged specimen. In specimens with a CFRP patch bonded with DP 420 adhesive (Figure 6a), plastic deformation of the specimen material outside the repair node occurred during loading - what meant that the repair node excessively stiffened the specimen in the repair zone. Plate deformation in plastic range outside the patch. In the case of large deformations of the loaded specimen, failure of the adhesive bond also occurred, but only when the repair patch was on the tensile side during bending of the specimen. (Figure 6b, Figure 7).

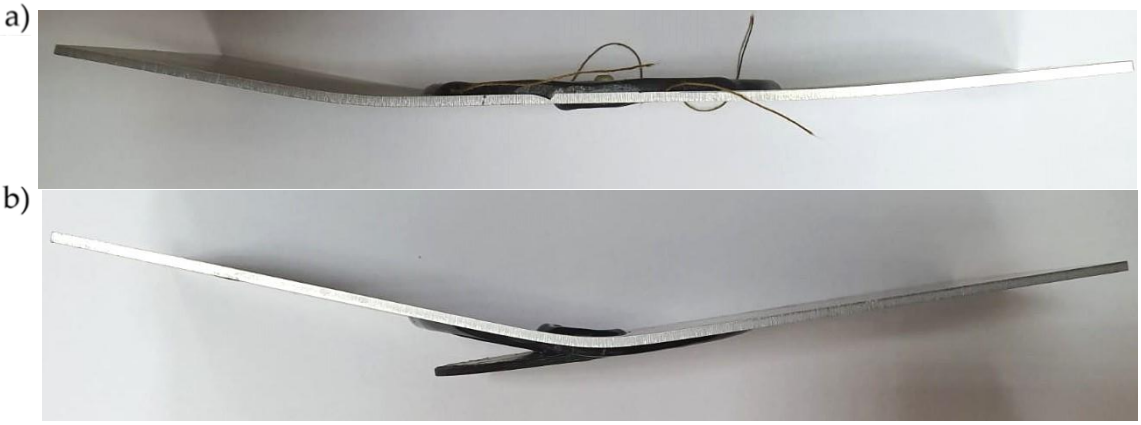

Fig. 6. Failure mode of specimens with CFRP patch: a) permanent deformation outside the repair node, b) failure of the adhesive joint

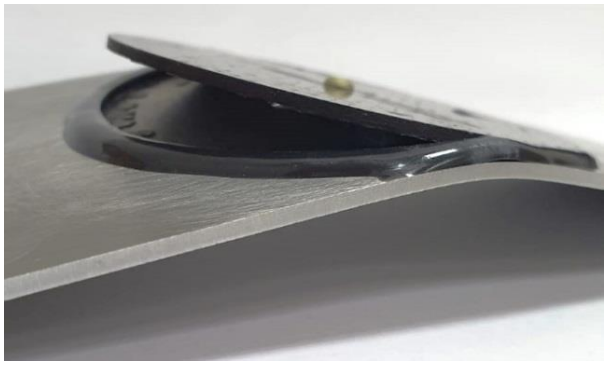

Fig. 7. Plastic deformation of the plate witch CFRP patch after loss of stability (failure of the adhesive joint)

The riveted patch specimen plastically deformed upon loss of stability (the deflection arrow was about 1.4 mm, but the riveted joint did not fail. The overlay made of 1 mm thick glass composite did not deform after the loss of stability of the loaded specimen. The patch deformed with the specimen without being damaged.

4. Numerical simulations

Using the finite element method and the computational capabilities of the CAE environment Ansys Workbench 2021R2 Static Structure module, the effect of the specimen geometry (its thickness and width) on the stress distributions occurring in the plate, patch and adhesive joint was analyzed. The calculations took into account the nonlinear properties of the AW-2024-T3 aluminum alloy by assuming a multilinear model of the material. The material constants of the DP 420 adhesive were determined experimentally during static tensile testing of the adhesive, Figure 8. Based on the $\sigma = (\sigma)\varepsilon$ curve of the DP 420 adhesive, the multilinear material properties of the adhesive were defined (Table 4). The nonlinear properties of AW 2024 T3 alloy are shown in Table 5. The properties of the composite material (GFRP) was defined as orthotropic with parameters presented in Table 6.

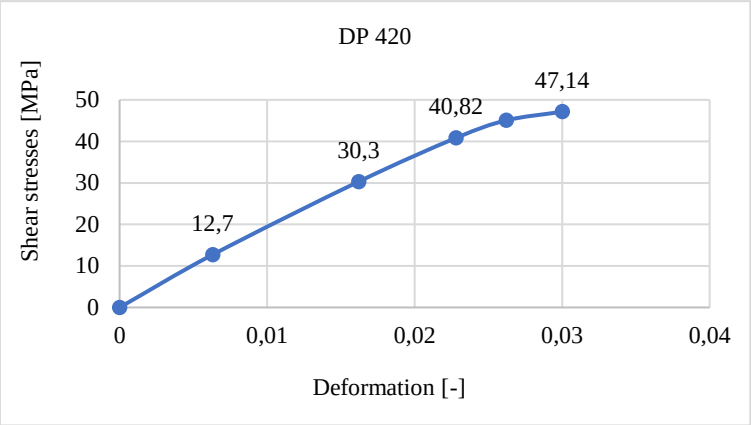

Fig. 8. σ = (σ)ε curve of DP 420 adhesive

Table 4. Strength parameters of DP 420 adhesive

Name of material	Young's modulus [GPa]	Poisson's ratio [-]	Strain [-]	Stress [MPa]
DP 420	2.083	0.35	0	1
			0.0063	12.7
			0.0162	30.3
			0.0228	40.82
			0.0262	45.05
			0.03	47.14

Table 5. Strength parameters of AW 2024 T3 aluminum alloy (Godzimirski and Pietras, 2012)

Name of material	Young's modulus [GPa]	Poisson's ratio [-]	Strain [-]	Stress [MPa]
AW 2024T3 NL	70	0.36	0	330
			0.0098	348.45
			0.0196	370
			0.0385	410.8
			0.0741	468.72
			0.1071	507.36
			0.1379	540.56

Table 6. Orthotropic properties of the composite patch

Name of material	Young's modulus [GPa]			Poisson's ratio [-]			Kirchhoff module [GPa]		
Direction	X	Y	Z	XY	YZ	XZ	XY	YZ	XZ
GFRP	15	15	5	0,04	0,3	0,3	3	2,2	2,2

Simulations were carried out for four design cases.

Case I – the geometric dimensions of the plate model were the same as the samples used in the experimental tests (Figure 9). The model was of an element of dimensions 150x80x2 mm (length, width, thickness) with a hole of 20 mm diameter. The defined specimen was shorter than the specimen used in the experiment due to the skip of the specimen surface located in the jaws of the testing machine - Figure 10. An insert with dimensions equal to the diameter of the hole was modeled in the hole. An adhesive joint with a diameter of 70 mm and a thickness of 0.15 mm and a composite patch with a diameter of 70 mm and a thickness of 1.6 mm were also modeled.

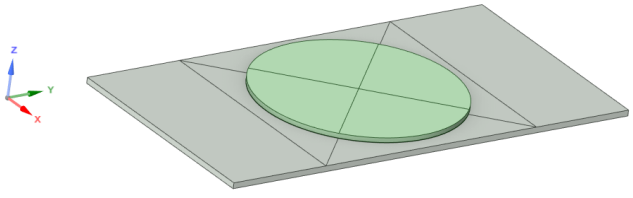

Fig. 9. The model of the repair node in the Geometry module

Using the *Contacts* function, the types of contacts occurring between the various elements of the model were defined. *Frictional* contacts with a factor of 0.1 were defined between the insert and the plate. *Bonded* contacts were defined between the adhesive joint and

the patch, the adhesive joint and the plate, and the adhesive joint and the insert [27].

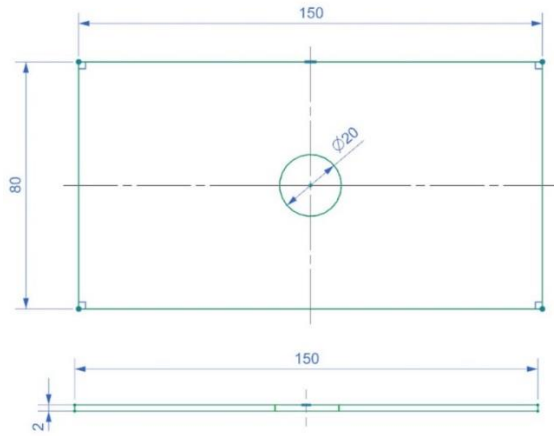

Fig. 10. Dimensions of the repaired plate

Discretization of the model was performed using the *Mesh* function. In the mesh parameters for the entire model, the *Mesh* elements were given a size of 2 mm. In order to obtain a hexagonal mesh, the *Multizone* function was used, defining the properties of a *Hexa*-type mesh. The *Edge Sizing* function was also used, and an element size of 1 mm was set on the edge of the hole. After the geometry was discretized, a model consisting of 4289 elements and 31162 nodes of Hex20 type was obtained.

Case II – The thickness of the plate was reduced from 2 mm to 1 mm. The plate had the following geometric dimensions: 150x80x1 mm (length, width, thickness);

Case III – the width of the plate was increased from 80 mm to 160 mm. The plate had the following geometric dimensions: 150x160x2 mm, (length, width, thickness);

Case IV – The width of the plate was increased from 80 mm to 160 mm and its thickness was reduced from 2 mm to 1 mm. The plate had the following geometric dimensions: 150x160x1 mm - (length, width, thickness).

In each case, the thickness of the composite patch was equal to 1.6 mm. Loads were defined by assuming that the stresses in the undamaged cross-section of the repaired panel should be equal to 220 MPa, which resulted from the yield strength of the material equal to 330 MPa and taking into account the safety factor equal to 1.5. Based on the value of the cross-section of each case, the maximum force was determined - Table 7.

Table 7. Load values for design cases

Case No.	Force kN
I	35.2
II	17.6
III	70.4
IV	35.2

The boundary conditions of the simulation were similar to those of the experimental test specimens - Figure 11. One edge of the model was fixed using *Displacement* (Dx, Dy, Dz = 0; Rx, Ry, Rz = Free), the opposite edge was fixed using *Displacement* (Dz = 0, Dy, Dx =Free; Rx, Ry, Rz = Free) and the tensile *Force* was modeled with the values shown in Table.

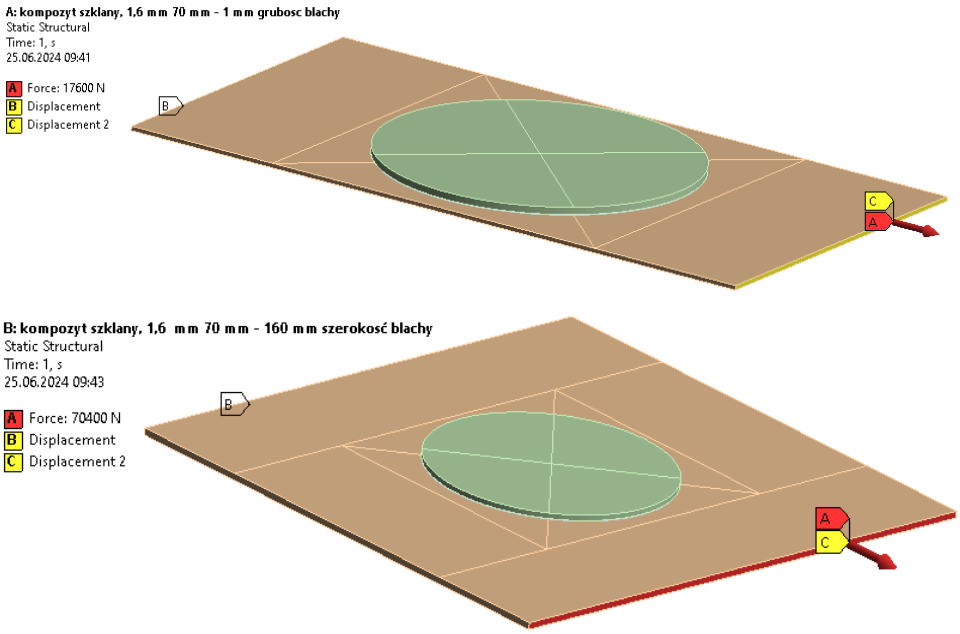

Fig. 11. Geometry and boundary conditions of case I and III

Example maps of reduced stresses according to the Huber-M-H hypothesis in plates for the four design cases are presented in Figures 12, 13, 14, 15, while Table 8 shows a summary of the maximum values of reduced stresses in the elements of the repair node.

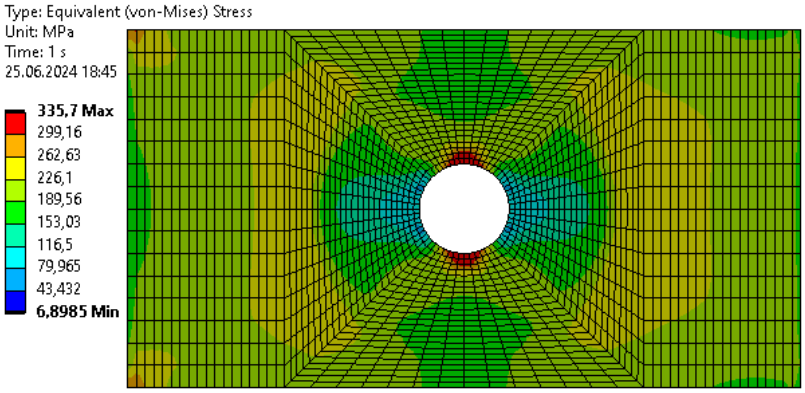

Fig. 12. Von-Mises stress map (Case I)

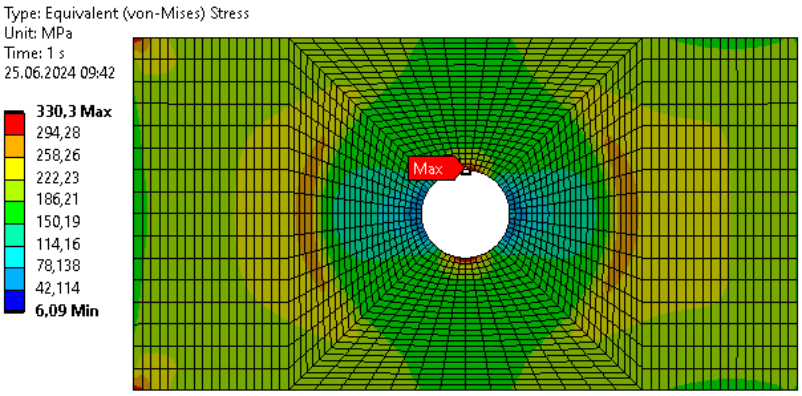

Fig. 13. Von-Mises stress map (Case II)

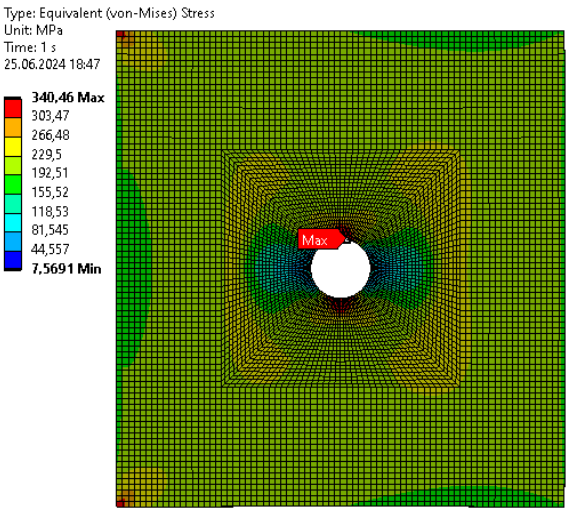

Fig. 14. Von-Mises stress map (Case III)

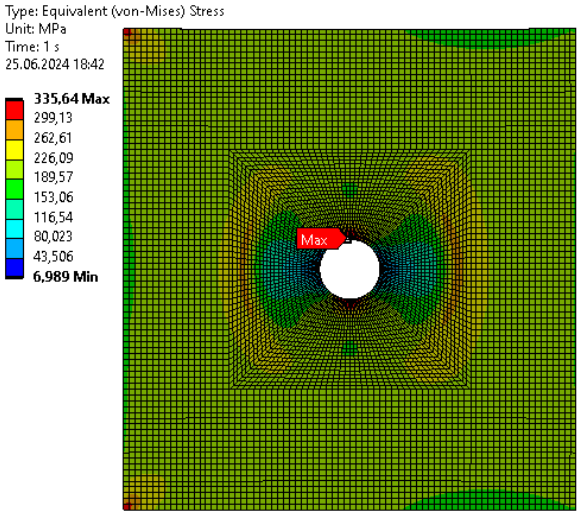

Fig. 15. Von-Mises stress map (Case IV)

Table 8. Results of numerical simulations of repair nodes

Calculation cases	Force kN	Maximum values of reduced stresses (von-Mises) [MPa]		
		Plate	Patch	Adhesive
Thickness 2 mm, width 80 mm	35.2	336.53	164.65	47.14
Thickness 1 mm, width 80 mm	17.6	334.48	92.35	30.44
Thickness 2 mm, width 160 mm	70.4	340.46	125.35	38.63
Thickness 1 mm, width 160 mm	35.2	335.64	98.36	30.74

The results of the numerical analysis show that the geometry of the model has an impact on the values of reduced stresses in both the adhesive joint and the patch. Significant differences in stress values are found in the composite patch (44%) and the adhesive joint (35%). Regardless of the analyzed changes in the geometry of the plate model, the maximum values of reduced stresses (according to the Huber -M-H hypothesis) in the repaired model are very close to each other (differences at the 1% level).

Taking into account the values of adhesive bond failure stresses of modern adhesive bonding materials, it follows that it is rational to repair thin metal skin by bonding composite patches. The positive effect of reducing stresses in adhesive joints was also observed for the case when the area of the repair zone is smaller in relation to the total area of the repaired specimen.

5. Conclusions

Based on experimental studies, it was concluded that:

- repairs using both riveted and bonded patches do not allow the restoration of the original tensile strength of the loaded skin, but allow the restoration of the compressive strength of the loaded skin (loss of stability);
- for elements of the skin where tensile loads on the material dominate, such as the lower part of the wing skin, stiffer patches (of greater thickness (1mm, 2 mm) or made of materials with higher stiffness - carbon-epoxy composite) should be used. It allows to reduce the stress level by 7.6% compared to the damaged one;
- for compression elements where loss of stability may occur, such as the upper part of the wing skin, patches with lower stiffness (thinner or, for example, made of glass-epoxy composite) are better.

The results of the numerical tests showed that:

- it is reasonable to repair only thin metal coverings by bonding composite patches due to the maximum stresses in the adhesive joints;
- there can be a reduction of stresses in the adhesive joints (35%) when the area of the repair node is smaller in relation to the total area of the repaired zone.

Acknowledgments

Funding: This work was financed by Military University of Technology under research project UGB 735/2024.

References

Achour T., Aid A., Albedah A., Bouanani M.F., Benyahia F., Bouiadjra B., Belhouari M., (2013). *Materials and Design* 50, 433-439.

Akash B., Apiccella A., Aversa R., Petrescu R., Bucinell R., Corchado J., Petrescu F. (2017). History of aviation - a Short review. *Journal of Aircraft and Spacecraft Technology*. 1 (1), 30-49.

Al-Rabeei S., Korba P., Hovanec M., Sekelová I., Kale U. (2024). Structural design and material comparison for aircraft wing box beam panel. *Heliyon*. Volume 10, Issue 5.

Albedah A., Bouiadjra B.A.B., Bouiadjra B.B., Benyahia F., Mohammed S.M.A.K., Mhamdia R. (2021). Fatigue crack growth in aluminum panels repaired with different shapes of single-sided composite patches. *Int. J. Adhes. Adhes*. 105, 102781.

Armstrong KB., Cole W.W., Bevan G. (2005) Care and repair of advanced composites. SAE International.

Ayedi H.F., Guermazi N., Haddar N., Elleuch K. (2014). Investigations on the fabrication and the characterization of glass/epoxy, carbon/epoxy and hybrid composites used in the reinforcement and the repair of aeronautic structures. *Materials*. 56, 714-724.

Azmin Shakrine, Prince Hasn, Mohd Rafie, Fairuz Izzuddin Romli. (2012). Modern design trend of metal aircraft fuselage structure. *International Science Postgraduate Conference 2012.* Volume 808-817.

Baker A. (1984). Repair of cracked or defective metallic aircraft components with advanced fibre composites – an overview of Australian work. *Composite Structures*. Volume 2, Issue 2, 153-181.

Baker A., Joned R. (1988). Bonded Repair of Aircraft Structures, *Martinus Nijhoff Publishers.*

Baker A. (1999). Bonded composite repair of fatigue-cracked primary aircraft structure. *Composite Structures*. Volume 47, Issue 1-4, 431-443.

Barca I., Rośkowicz M. (2022). Analysis of the airframe repair node. *Assembly Techniques and Technologies.* 3/2022, 42-48.

Barca I., Godzimirski J., Rośkowicz M. (2023). Selection of materias for repairing punctures of metal skin of semimonocoque structures using composite patches.

Assembly Techniques and Technologies. Volume 120, Issue 2/2023, 19-32.

Bazargan M. (2010). Airline operation and scheduling. *Ashgate Publishing Limited*, Farnham.

Bond D., Davis M. (1999). Principles and practices of adhesive bonded structural joints and repairs. International Journal of Adhesion and Adhesives. Volume 19, Issues 2-3, 91-105.

Chang R.C., Zang S. (2023). Structure health inspection for aging transport aircraft. *Aircraft Engineering and Aerospace Technology*.

Camanho P.P., Matthews F.L. (1999). A progressive damage model for mechanically fastened joints in composite laminates. Journal of Composite Materials. 33 (24), 2248--2280.

Camanho P.P., Lambert M. (2006). A design methodology for mechanically fastened joints in laminated composite materials. *Composites Science and Technology*. 66 (15), 3004-3020.

Cantwell W.J., Morton J. (1992). The significance of damage and defects and their detection in composite materials: a review. *The Journal of Strain Analysis for Engineering Design*, 27 (1), 29-42.

Dai J.T., Zhao P.Z., Su H.B., Wang Y.B. (2020). Mechanical Behavior of Single Patch Composite Repaired Al Alloy Plates: Experimental and Numerical Analysis. *Materials*. 13, 2740.

Gan, Salehi-Khojin, Zhamu; Zhong. (2006). Effects of patch layer and loading frequency on fatigue fracture behavior of aluminum plate repaired with a boron/epoxy composite patch. *J. Adhes. Sci. Technol*. 20, 107-123.

Godzimirski J., Pietras A. (2012). Numerical strength analysis of hybrid sandwich composites. *WAT Bulletin.* Vol. LXI, Nr 3.

Gunnion A.J., Wang C.H. (2009). Optimum shapes of scarf repairs. *Composites Part A Applied Science and Manufacturing*, 40 (9), 1407-1418.

Hamill L., Nutt S. (2018). Adhesion of metallic glass and epoxy in composite-metal bonding. *Composites Part B: Engineering.* Volume 134, 186-192.

Henaff G., Renon V., Larignon C., Perusin S., Villechaise P. (2019) Identification of Relationships between Heat Treatment and Fatigue Crack Growth of alpha beta Titanium Alloys. *Metals*. 9, 512.

Hoff N.J. (1946). A Short History of the Development of Airplane Structures. *Journal Article.* Volume 34, No. 3, 370-388.

Katnam K.B., Da Silva L.F.M., Young T.M. (2013). Bonded repair of composite aircraft structures: A review of scientific challenges and opportunities. *Progress in Aerospace Sciences*. Volume 61, 26-42.

Khazaei M., Mohammadi S., Yousefi M. (2021). A review on composite patch repairs and the most important parameters affecting its efficiency and durability. *J. Reinf. Plast. Compos.* 40, 3-15.

Kołodziejczyk R., Święch Ł. (2018). Mechanics in Aviation ML-XVIII 2018 Stiffness study of thin-walled composite wing structure of unmanned aircraft. *Polish Society for Theoretical and Applied Mechanics.*

Lee H., Seon S., Park S., Walallawita R., Lee K. (2021). Effect of the geometric shapes of repair patches on bonding strength. *J. Adhes*. 97, 207-224.

Ma L., Zhou W., Ji X., Yang S., Liu J. (2021). Review on the performance improvements and non-destructive testing of patches repaired composites. *Composite Structures.* 263. 113659.

Megueni A., Yala A.A. (2009). *Materials and Design.* 30(1), 200-205.

Motley George Ronald. (1980). A Study Of The Reinforcement Required For Cutouts In Aircraft Semi-monocoque Structure. *Southern Methodist University ProQuest Dissertations & Theses.* 8012578.

Prakash M.B., Ramji M., Srilakshmi R. (2013). Towards optimization of patch shape on the performance of bonded composite repair using FEM. *Compos. Part B Eng*. 45, 710-720.

Rośkowicz M., Smal T. (2012). The use of composite materials to repair of aircraft semi-monocoque aircraft semi-monocoque airframes. *ECCM15 – 15th European Conference on Composite Materials.*

Shazly Mostafa. (2021). Improvement of scarf repair patch shape for composite aircraft structures. *The Journal of Adhesion*. 1044-1070.

Siddiqui Tariq. (2014) Aircraft Materials and Analysis. *McGraw Hill Education*. Page 9.